Parallel RF Transmission based MRI Technique for Highly Sensitive Detection of Amide Proton Transfer in the Human Brain at 3T

J. Keupp[1], C. Baltes[2], P. R. Harvey[2], and J. van den Brink[2]
[1]Philips Research Europe, Hamburg, Germany, [2]Philips Healthcare, Best, Netherlands

Introduction

Amide proton transfer (APT) MRI for the *in vivo* detection of endogenous cytosolic proteins or peptides [1] is enabled by chemical exchange between amide protons (3.5 ppm) and the bulk water. The signal of amide proton transfer (APT) reflects protein concentrations as well as local pH via the exchange rate. Promising clinical applications of APT-MRI are envisioned in oncology (enriched protein levels in tumors [2]) and in neurology (ischemic acidosis in stroke patients [1]). Ideally, a RF saturation duration of t_{sat}>2 sec is needed to achieve 90% of the possible APT ratio, because it scales with $APTR=APTR_{\infty}(1-\exp(-R1_w \times t_{sat}))$ [3], where $APTR_{\infty}$ is the asymptotic transfer ratio for $t_{sat}\rightarrow\infty$ and $R1_w \approx 1$ sec is the water relaxation. While successful APT applications have been shown in the human brain [4,5], saturation was typically limited to $t_{sat} \leq 800$ ms due to RF amplifier specifications (maximum pulse length and duty-cycle) in the clinical systems, and only about 50% of the maximum APTR could be achieved. Herein, a novel scheme for prolonged RF saturation is demonstrated for APT-MRI, which is applicable to state-of-the-art clinical MR systems equipped with whole-body parallel transmission capability. Sequence variants are assessed for optimal sensitivity, and feasibility of APT mapping in the human head is demonstrated.

Methods

The study was performed on a 3.0T clinical whole-body scanner (Achieva 3.0T TX, Philips Healthcare, NL) using an 8-channel head coil for signal reception as well as the parallel transmission sub-system and body-coil for RF transmission. Acquisition software was modified to operate the two RF amplifiers of the system in an alternating fashion during the RF saturation pulse (Fig. 1). Thus, each amplifier can be operated at full power, while staying within the specified duty-cycle of 50% and maximum pulse length. Imaging pulses were RF shimmed for spatial homogeneity, while the independent channels were driven with equal amplitudes for the RF saturation pulse. An alternated saturation pulse-train of 3 sec was used (48 × 62.5 ms, Sinc-Gauss shape), $B_{1,rms}$=1.8 μT, head SAR_{max}=3 W/kg. 6 saturation off-resonance frequency points S[ω] in steps of 0.63 ppm around Δω=±3.5 ppm (APT) and one far off-resonant (S_0, Δω=-160 ppm) were recorded. Three 2D sequence types were compared for optimal sensitivity in terms of contrast-to-noise ratio (CNR): (i) segmented dual-echo GRE, (ii) fast spin-echo (TSE) and (iii) driven-equilibrium [6] (DRIVE) with the following parameters: FOV (220 mm)^2, matrix 144^2, resolution 1.5×1.5×6 mm^3, and 3 minutes scanning time. For (i), 2 echoes were acquired in 4 segments with TS=6070 ms per off-resonance and TR=9.5 ms, TE_1=2.7 ms, TE_2=6.6 ms, pixel bandwidth (pBW) 290 Hz, α=30°, whereas for (ii)&(iii), 4 shots with TR=6130 ms, TE=6.4 ms, α=90° and pBW=300 Hz were used. From (i), δB_0 maps could be calculated by iterative Dixon reconstruction [5] and used for all off-resonance corrections. Images at different frequency offsets were co-registered using rigid-body translations to compensate for head motion. Maps of the asymmetric amide proton transfer ratio $APTR=(S[-3.5ppm]-S[+3.5ppm])/S_0$ were calculated based on δB_0 corrected, point-by-point interpolated images S[-3.5ppm] and S[+3.5ppm]. CNR=APTR/σ[APTR] based sensitivity assessment was performed on a protein phantom with 5 different concentrations (7…70%) of chicken egg-white diluted with H_2O. *In vivo* feasibility was tested in a human volunteer, from whom informed consent was obtained.

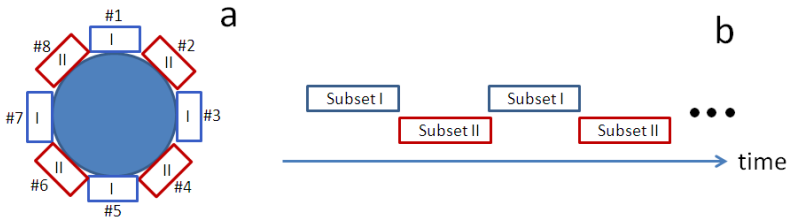

Figure 1: Schematic representation of multi-element transmit based RF saturation for APT-MRI: The transmit channels are divided in two subsets or modes I/II (a) which are driven by the RF amplifiers in a time-interleaved fashion (b), thus running each amplifier at 50% duty-cycle and limited pulse duration according to their hardware specifications.

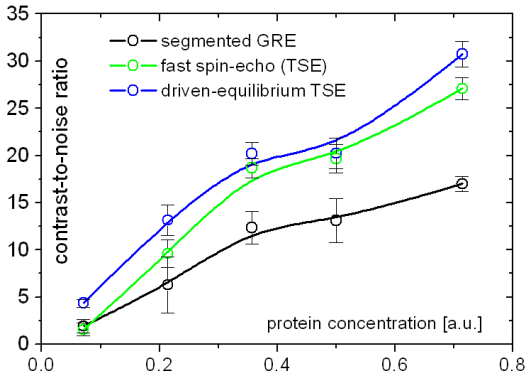

Figure 2: Sensitivity assessment of APT-MRI techniques with 3 sec of multi-transmit based RF saturation in terms of CNR for varying concentrations of a protein phantom (egg-white): Fast spin-echo techniques are superior to GRE and a driven-equilibrium (DRIVE) sequence offers highest sensitivity, in particular at low protein concentrations.

Results and Discussion

Time-interleaved parallel transmission based APT-MRI was successfully demonstrated *in vitro* and *in vivo*. Fast spin-echo based APT showed superior sensitivity compared to the GRE technique (Fig. 2). In particular at low protein concentrations, the driven-equilibrium technique offered up to a 2-fold enhancement of CNR and thus should be considered for clinical APT applications. To demonstrate *in vivo* feasibility, the driven-equilibrium based results are shown in Figure 3. The point-by-point interpolated images S[-3.5ppm] (a) and S[+3.5ppm] (b) yield a flat APTR baseline after δB_0 correction (c), while before correction, considerable inhomogeneity was observed (d). The net RF saturation by alternated channel subsets results in a homogeneous baseline saturation effect, upon which an increased protein content (e.g. of a tumor) could be detected with high sensitivity. Further *in vivo* studies on tumor patients are needed to validate the CNR gain obtained by increasing the saturation pulse length via the parallel-transmission technique and by using the driven-equilibrium fast spin-echo acquisition. A 3D coverage of the brain, often required in brain oncology applications, would be possible by combination with a gradient-and-spin echo readout (GRASE) [5].

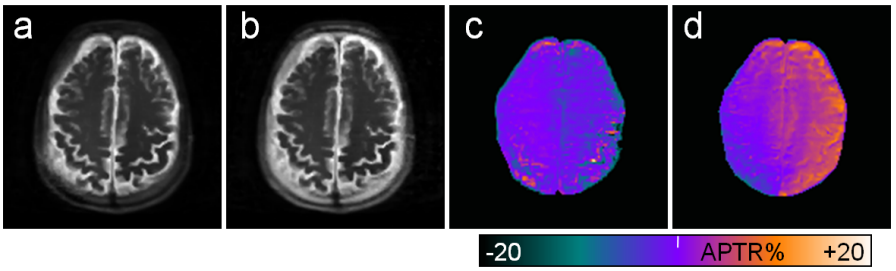

Figure 3: Results from a multi-element transmission based 2D driven-equilibrium APT-MRI sequence on a healthy volunteer: (a) RF saturation at -3.5 ppm, (b) +3.5ppm, (c) APTR baseline measurement, (d) APTR without δB_0 correction.

References

1. Zhou J et al., Nat Med 9:1085 (2003)
2. Jones CK et al., MRM 56: 585 (2006)
3. Howe FA et al., MRM 49:223–232 (2003)
4. Zhou J et al., MRM 60:842 (2008)
5. Zhu H et al., MRM 64:638-44 (2010)
6. Becker ED et al., J Am Chem Soc 91:7784 (1969)